JOURNAL OF MATERIALS SCIENCE 29 (1994) 4216–4224

Surface laser treatment of ductile irons

V. LOPEZ, J. M. BELLO, J. RUIZ and B. J. FERNANDEZ
CENIM (CSIC), Avda Gregorio del Amo, 8 E-28040 Madrid, Spain

The effect of the laser surface treatment of three types of ductile iron (Grades 60–40–18, 80–55–06 and 100–70–03) was studied. Using a continuous CO_2 laser with a square 10 mm × 10 mm beam and uniform power density, the effect of beam scan rate at 2.5 and 5 kW power output was investigated. At each power rate, a range of scan rates was used to produce treatments with and without surface melting. The microstructure and hardness of the different zones of the treated material were analysed. It was found that layers of white iron of the same depth were produced in the three test irons when the operating conditions melted the surface material. Surface porosity can be eliminated by melting, although transverse cracks appeared on the surface with this treatment. Surface martensitic hardening produced a layer of uniform hardness only in the case of the grade 100–70–03 ductile iron with a perlitic matrix.

1. Introduction

Ductile irons have a wide range of applications. They have advantages for casting manufacture, and have good machinability. These characteristics vary considerably depending on whether they have ferritic, perlitic or mixed matrix microstructure.

Surface laser treatment of ductile irons [1–6] allows a high level of hardness to be attained on the surface of the materials. This may be achieved by martensitic hardening when the matrix is perlitic, or by surface melting. Undoubtedly, the surface treatment of ductile iron makes a notable improvement to the wear resistance of the product [7, 8] but may decrease its fatigue performance [2, 9].

The present work analysed the structural and hardness changes caused by CO_2 continuous laser treatment of different types of ductile irons, and the potential appearance of defects in the material.

2. Material and methods

In the study, three types of ductile iron were used, classified by their mechanical characteristics into grades 60–40–18, 80–55–06 and 100–70–03 of ASTM A536. Fig. 1 shows the previous microstructures of the three ductile irons. The microstructure of the 60–40–18 ductile iron is composed of graphite nodules in a matrix of free ferrite. Ductile iron 80–55–06 exhibits a structure of graphite nodules in a perlitic–ferritic matrix, with a ferrite proportion of approximately 50%. The microstructure of perlitic iron 100–70–03 consists of graphite nodules surrounded by free ferrite (a bulls-eye structure) in a perlitic matrix.

Cast plates of 300 mm × 195 mm × 25 mm were used to prepare 45 mm × 23.5 mm × 22 mm parallelepipedic samples for the surface laser-treatment experiments. The treatments were carried out successively on the three test materials with a single sweep of the laser beam along the longitudinal axis of the 45 mm × 23.5 mm faces, which were previously spray covered with matt black paint.

The laser treatment involved a 10 mm × 10 mm square beam of uniform power density generated by a continuous CO_2 laser of 5 kW output power. Table I indicates the operating conditions, output power and scan rate during the tests. According to previous estimates [10], power outputs of 5 and 2.5 kW correspond to effective power densities of 2.6 and 1.6 kW cm^{-2}, respectively.

The results of the laser treatment were analysed by means of microscope examination of transverse cross-sections of the treated zones, and the determination of Vickers hardness (HV0.5) at different depths. The 45N Rockwell hardness of the treated surface was also determined.

3. Results

Case hardening and surface melting may be obtained with the operating conditions of Table I.

The direct measurement of hardness on the treated surface show that the hardening produced by surface treatment depends on the ductile iron type.

Fig. 2a and b show variations in Rockwell hardness 45N according to the scan rate when operating with output powers of 2.5 and 5 kW, respectively. The highest levels of hardness (68–76 HR 45N, equivalent to 61 and 68 HRc) were obtained for scan speeds corresponding to the surface melting of the sample. When melting was attained, the highest hardening was produced on the ferritic ductile irons, while the ferritic–perlitic and perlitic irons were somewhat lower. Relatively high levels of surface hardness were obtained in the perlitic iron for scan speeds that permit the martensitic hardening of the perlitic matrix. However, in the ferritic and ferritic–perlitic matrix nodular irons, the hardness level fell sharply when the

0022–2461

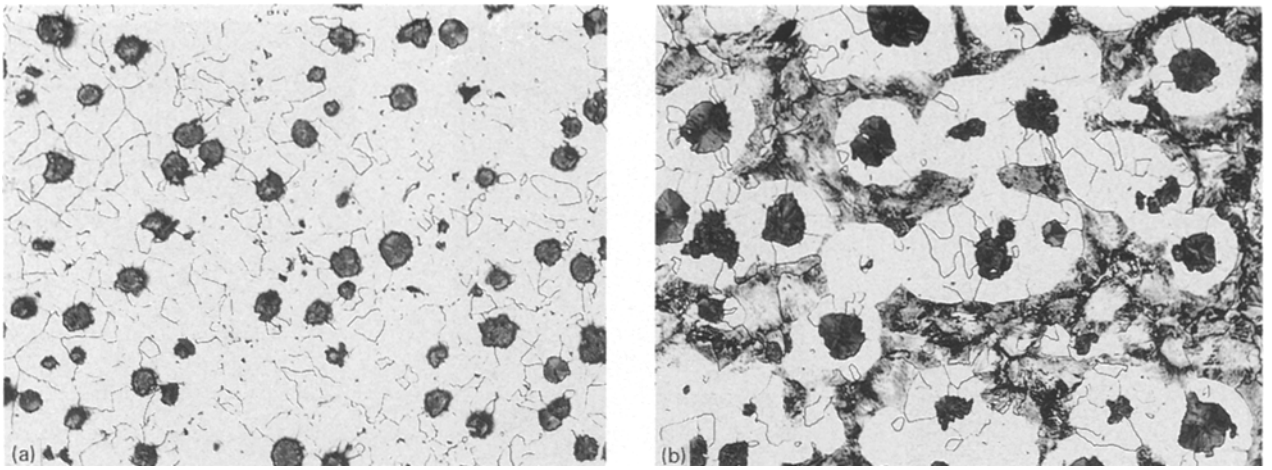

Figure 1 Microstructures of the (a) 60–40–18, (b) 80–55–06 and (c) 100–70–03 ductile irons. × 100

TABLE I Operating conditions of the tests

Output power (W)	Scan rate (m min^{-1})							
5000	1	1.15	1.44	1.88	2.5	3.6	4.35	5.95
2500	0.3	0.5	0.575	0.7	1	1.15	1.44	1.8

scan speed reached levels that no longer permitted surface melting.

Fig. 3 illustrates the microstructure of the ferritic ductile iron layers treated with a 5 kW beam at speeds of 1, 1.15 and 1.44 m min^{-1}. Surface melting occurred in all three cases. The molten layer still conserves remnants of nodules that were not fully dissolved. Melting can be seen to have commenced in the material surrounding the graphite nodules. Below the molten layer, martensitic hardening only occurred in the zones near the graphite nodules, impeding a proper hardened zone beneath the molten zone.

Fig. 4 shows the changes in the microstructure as a consequence of the laser treatment. Initially (a), the nodule was surrounded by ferrite. Where the heating temperature was sufficiently high (b), the nodule began to release carbon to the zone surrounding it, which hardened to martensite. More intense heating (c) caused the material near the nodule to start melting. Melting progressed as the temperature rose (d), and a rapidly solidified hypoeutectic structure with graphite nodules appeared. In the zone where the temperature attained was very high (e), the graphite nodules dissolved totally in the molten pool, and a eutectic type of solidification structure was produced. The white iron was composed of cementite, martensite and retained austenite. An occasional nodule of graphite may appear trapped in the melted zone.

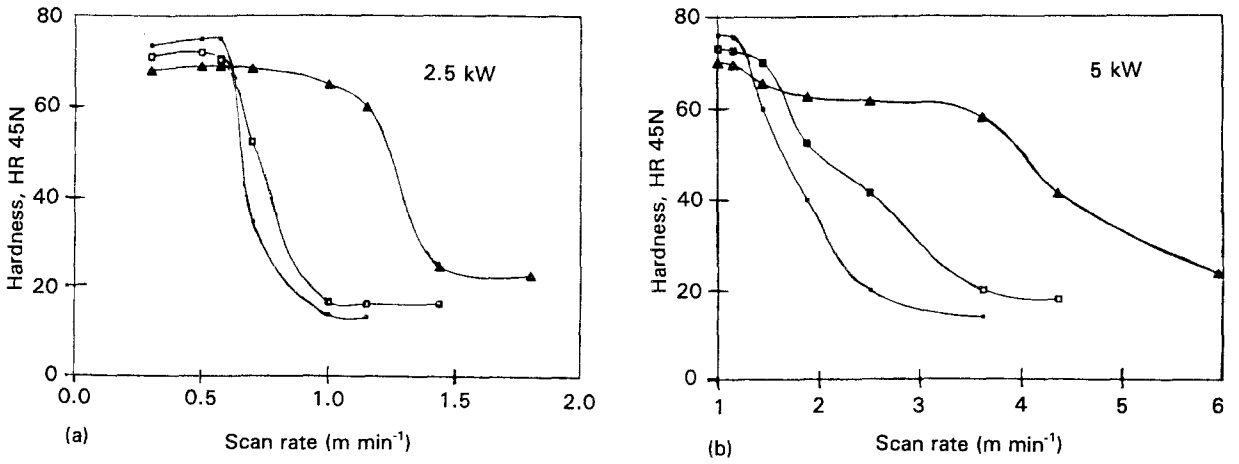

Figure 2 Surface hardness in the three ductile irons for two output powers as a function of the laser scan rate. (a) 2.5 kW, (b) 5 kW. (●) 60–40–18, (○) 80–55–06, (▲) 100–70–03.

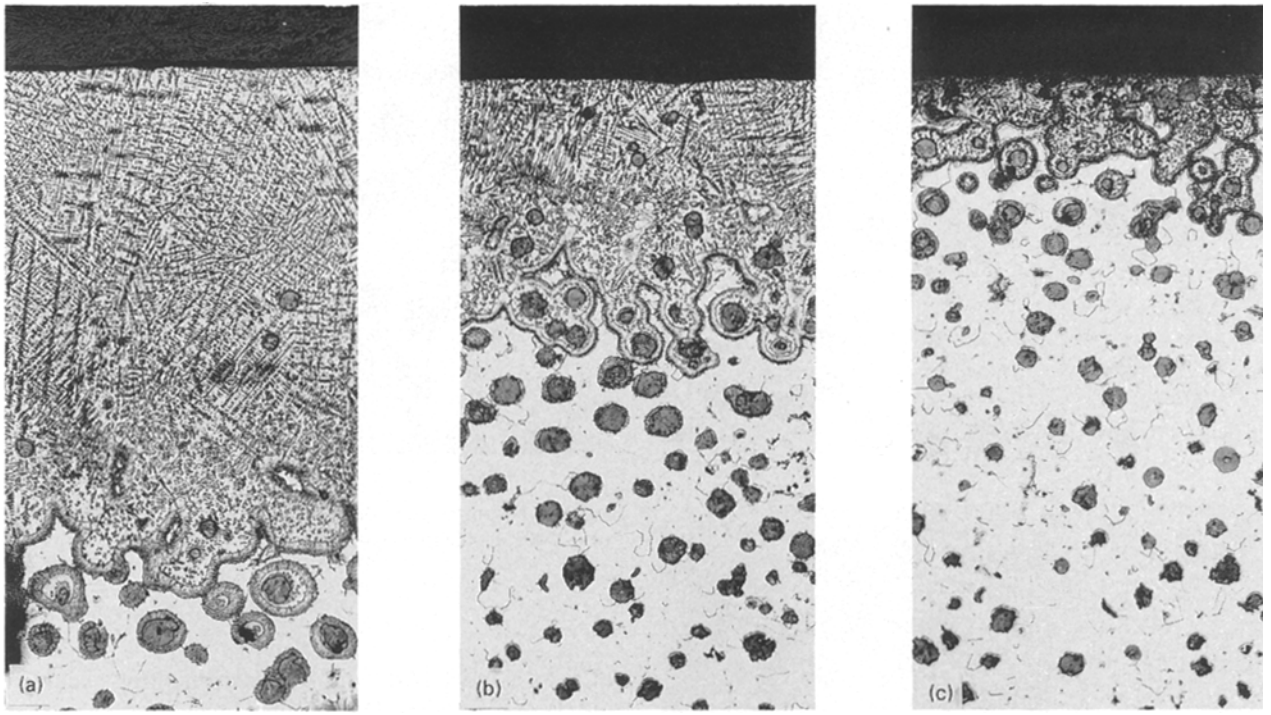

Figure 3 Microstructure of the molten layers in the ferritic ductile iron for 5 kW output power and (a) 1, (b) 1.15 and (c) 1.44 m min^{-1} scan rates. × 63

Fig. 5 shows the variation in hardness (HV0.5) with depth when the ferritic ductile iron has been treated with a 5 kW beam at a scan speed of 1 m min^{-1}. The graphite nodules were avoided during hardness measurement. Moving from the melt zone to unmelted material, there was a sharp fall in hardness as the ferrite matrix did not transform into martensite. A homogeneous layer of white iron with an HV0.5 hardness of 1040 was obtained. In the 2.5 kW beam treatments, the hardness of the molten layer was 1010 HV0.5. The higher power treatment led to a finer structure in the solidified material.

The perlitic ductile iron responded to the laser treatment in a different manner from the ferritic ductile iron, solely because of the presence of the perlite in the matrix. Fig. 6 shows the microstructures obtained in the former type treated with a 5 kW beam and several scan speeds. At the lowest scan rate (1 m min^{-1}), the molten layer had a depth of 0.63 mm with no graphite nodules near the surface. These began to appear in the molten layer from a depth of 0.25 mm onwards. The martensitic hardened zone continued inwards to 1.74 mm. The initial ferrite disappeared around the nearest to the molten area graphite nodules.

At a scan speed of 1.44 m min^{-1}, melting continued but some undissolved graphite nodules remained, even on the surface of the molten layer. The hardened zone was thinner. At 2.5 m min^{-1}, melting only took place in isolated zones of the surface near the graphite nodules. At scan speeds of 3.6 m min^{-1} or more, melting did not occur and only a zone hardened to

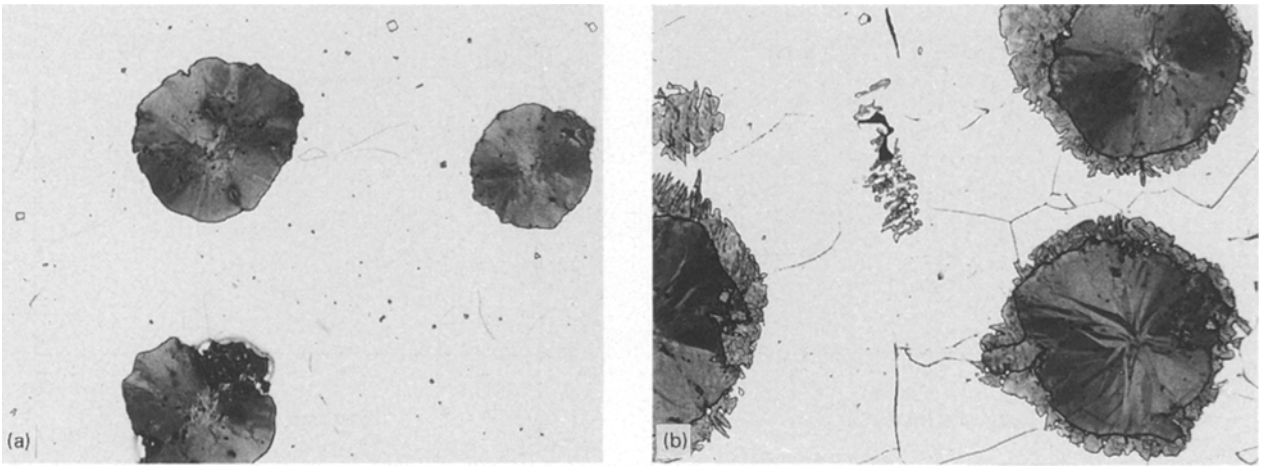

Figure 4 Effect of the laser treatment on the ferritic ductile iron microstructure. × 500

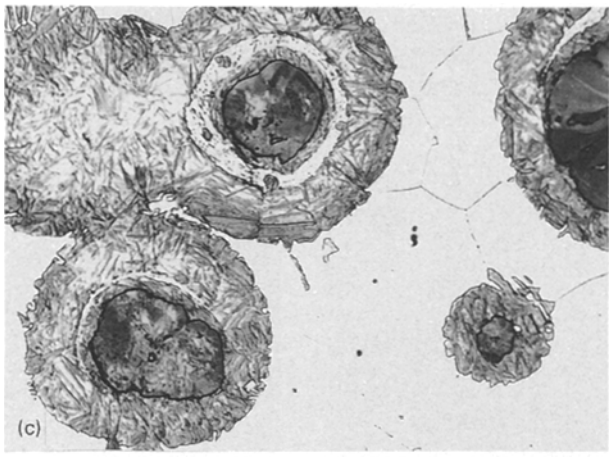

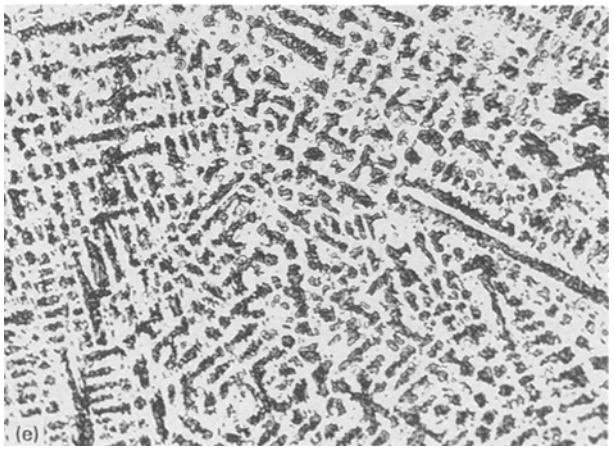

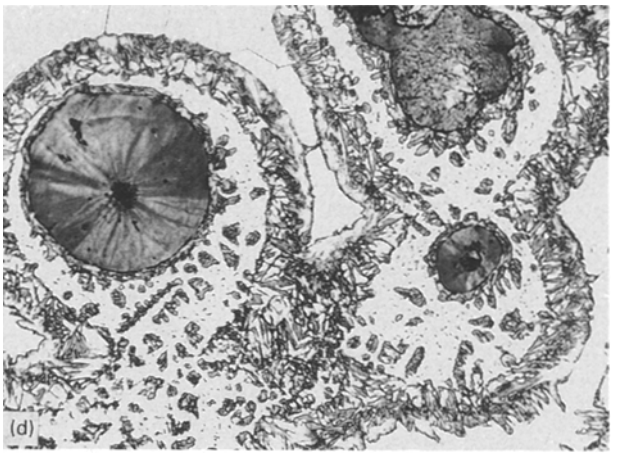

Figure 4 Continued.

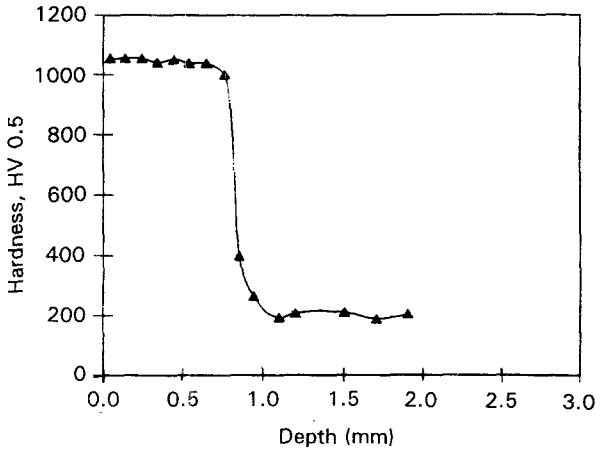

Figure 5 Hardness profile in the ferritic ductile iron 60–40–18 treated with 5 kW output power at a scan speed of 1 m min^{-1}.

martensite appeared on the surface. Under these conditions, there were always graphite nodules on the surface.

The micrographs in Fig. 7 illustrate the evolution of the microstructure in the perlitic ductile iron during laser treatment. Initially (a), the graphite nodule was surrounded by ferrite in a matrix of lamellar perlite. Wherever the heating temperature was high enough (b), the perlite was transformed into martensite. In this case, the resultant martensite was heterogeneous, because the perlite carbide was not fully dissolved in the austenite phase. At very high temperatures (c), there was a diffusion of carbon of the graphite in the austenite formed from the ferrite, and the dissolution of the cementite in the austenite was completed. The ferrite thus began to disappear, and the martensite resulting from the perlite became more uniform. At a higher temperature (d), prior to melting, the ferrite disappeared totally and a microstructure of spheroid graphite and martensite was obtained. Subsequently (e), an austenite with a high carbon content was produced around the graphite and local melting began. The molten material underwent hypoeutectic solidification and the graphite nodule was surrounded by needles of martensite in a matrix of retained austenite. The complete dissolution of the graphite in the molten layer (f) led finally to a structure of eutectic solidification, composed of iron carbide, martensite and retained austenite.

The hardness curves (Fig. 8), represent the variation in hardness through depth for two states of treatment of the perlitic ductile iron. The upper curve is a melting treatment with a 5 kW beam and a scan rate of 1 m min^{-1}. Three zones can be distinguished: the molten area with a hardness of 1010 HV0.5, the hardening zone of 860 HV0.5, and the untreated perlite substratum (380 HV0.5).

The lower curve corresponds to a treatment without melting at a beam intensity of 2.5 kW and a 1.15 m min^{-1} scan rate. This curve only has two zones: a hardened area (860 HV0.5) and the untreated substratum.

By the laser treatment of the nodular ductile iron with a mixed ferritic–perlitic matrix, intermediate results are obtained between those of the ferritic and perlitic irons.

When this mixed ductile iron was treated with a 5 kW beam and a scan rate of 1, 1.15 and 1.44 m min^{-1} (Fig. 9), a molten zone was obtained that contained residues of the graphite nodules. Beneath the molten zone there were portions of material that hardened to martensite and largely came from the perlite that was initially present. Some martensite also appeared beside the graphite nodules and the unaffected ferritic formations. At 2.5 m min^{-1}, only a few points of the surface were melted. Melting began

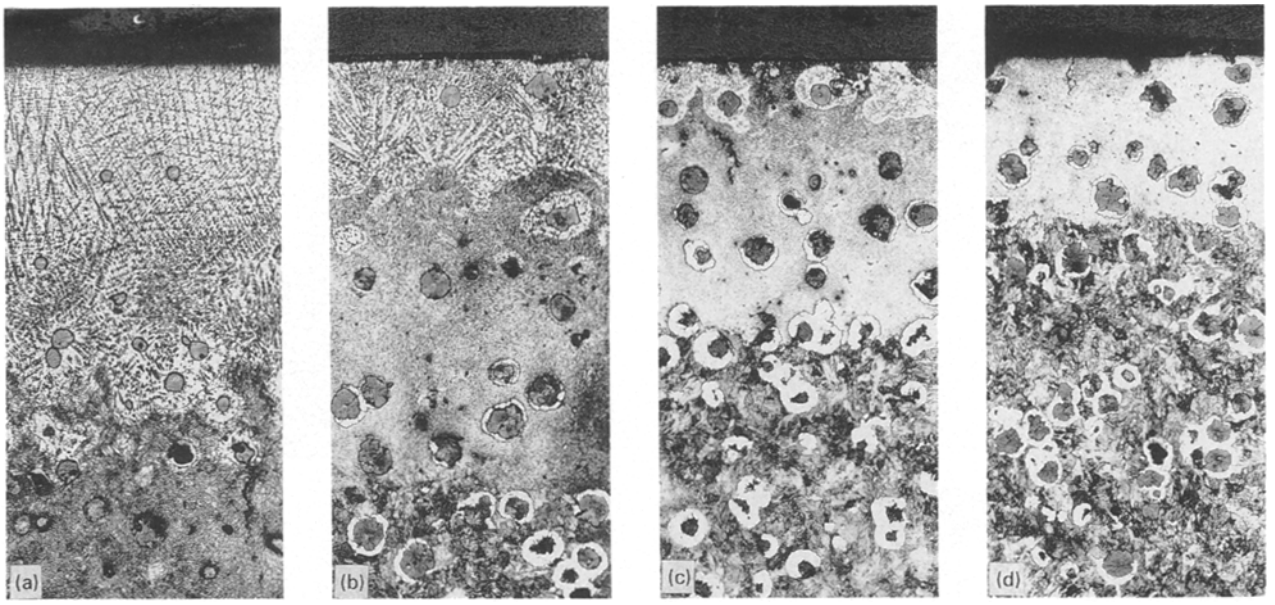

Figure 6 Microstructure of the treated zone in the perlitic ductile iron for 5 kW output power and (a) 1, (b) 1.44, (c) 2.5 and (d) 3.6 m min^{-1} scan rates. × 63.

before all of the austenite from the ferrite was enriched in carbon through the dissolution of the graphite nodules. A martensite layer covering the whole surface was thus not produced.

In the ferrite–perlite matrix iron treated with a 2.5 kW beam, the hardness of the white iron was 1040 HV0.5. The hardness of the martensite from the formerly perlite zones was 850 HV0.5.

Along with these martensitic zones, there were others with a soft ferrite structure (210 HV0.5). Thus,

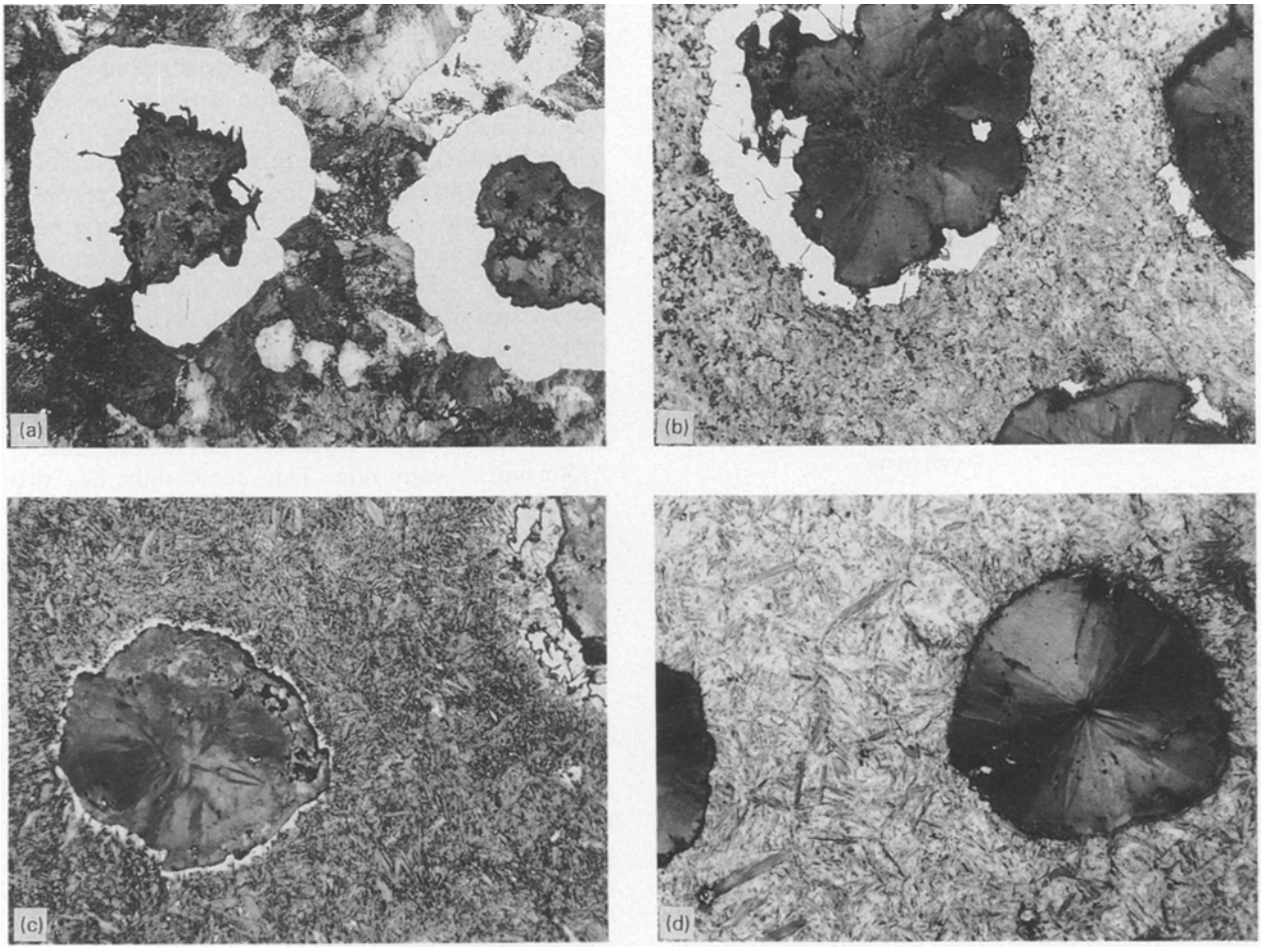

Figure 7 Effect of the laser treatment on the perlitic ductile iron microstructure. × 500

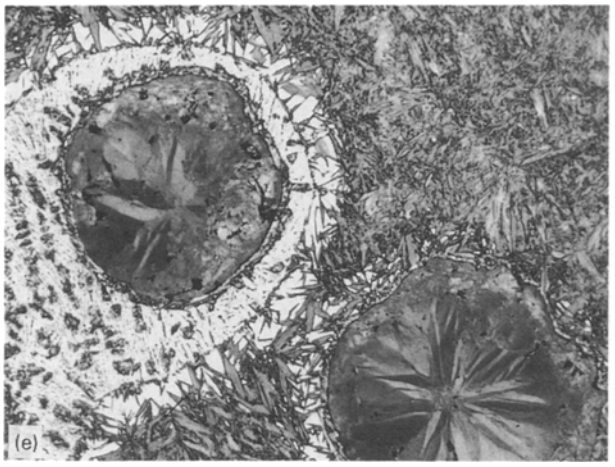

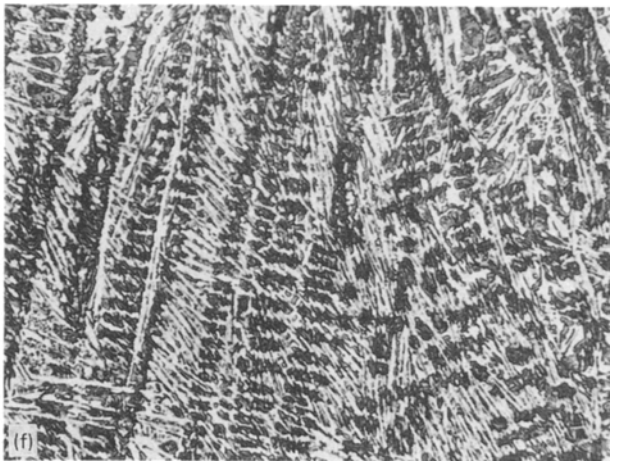

Figure 7 Continued.

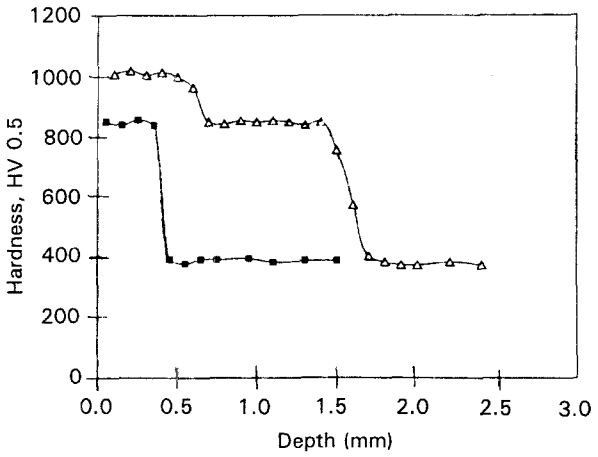

Figure 8 Hardness profiles in the perlitic ductile iron 100–70–03 treated for two working conditions. (△) 5 kW output power and 1 m min^{-1} scan rate, (■) 2.5 kW and 1.15 m min^{-1}.

in the ferrite–perlite matrix iron, a stable level of hardness was only obtained on the white iron layer. Beyond the molten layer, the thermally affected layer varied in hardness between the levels of the martensite and those of the initial ferrite.

Fig. 10 indicates the depths of the molten layer (F) and of the zone hardened to martensite (M) according to scan rates for the three studied materials when operating with a 2.5 and 5 kW beam. As a result of the surface treatment of the ferritic ductile iron (Fig. 10a and b), the depth attained by the molten zone (F) was considered according to the scan rate. The experimental points marked on the X-axis indicate the operating conditions under which only local melting was found around the graphite nodules.

In the case of the ferritic–perlitic ductile iron (Fig. 10c, d), one can distinguish between a molten

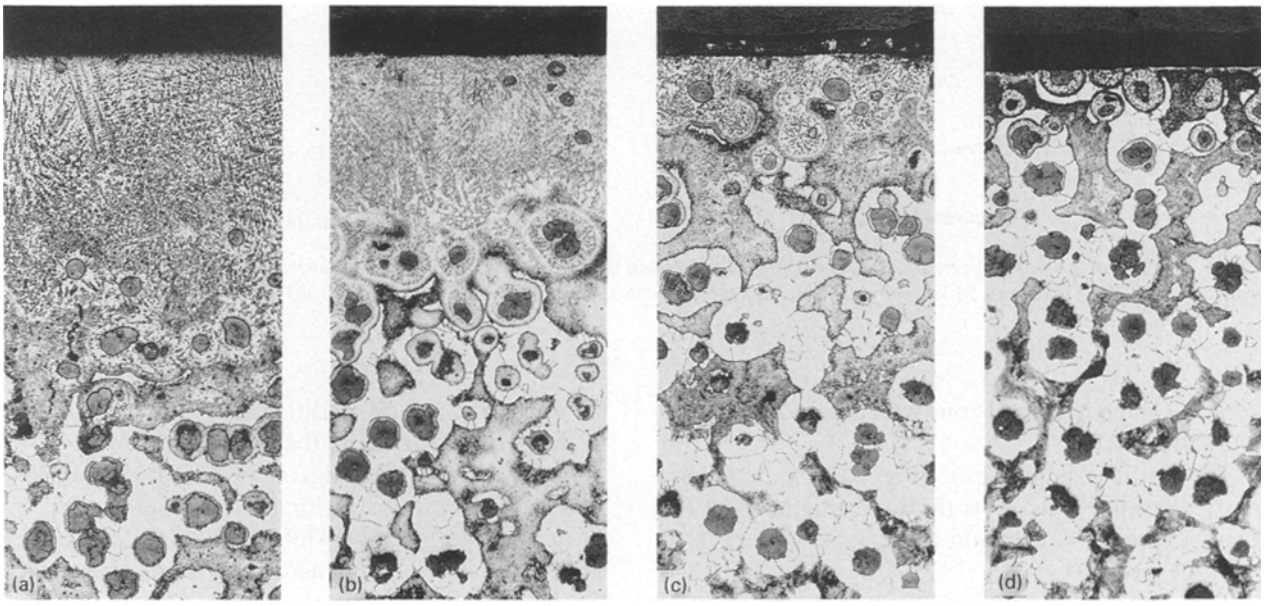

Figure 9 Microstructure of the treated zone in the ferritic–perlitic ductile iron for 5 kW output power and (a) 1, (b) 1.15, (c) 1.44 and (d) 2.5 m min^{-1} scan rates. × 63

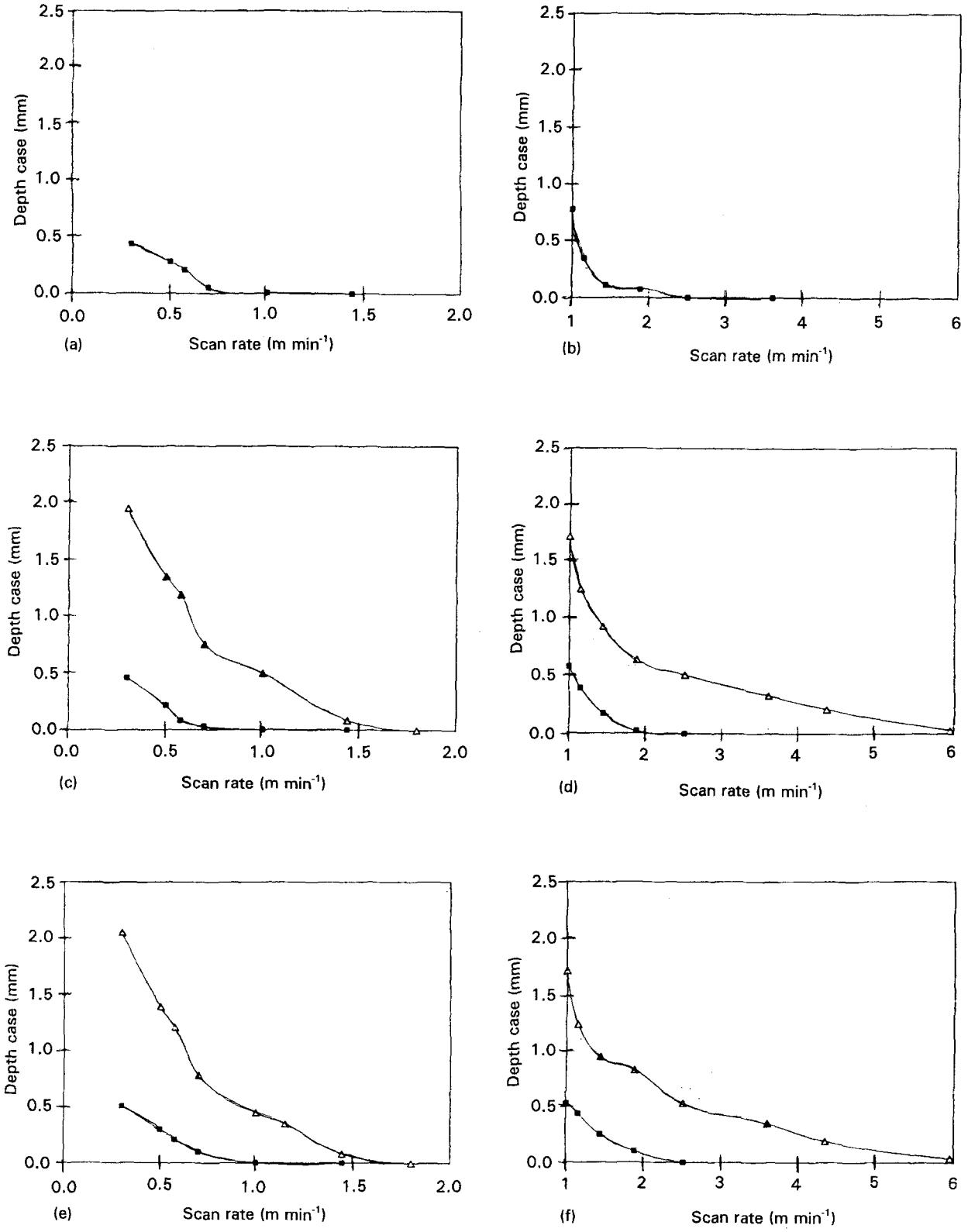

Figure 10 Effect of the working conditions on the depths of the molten layer (F) and of the martensitic hardened zone (M) in the three ductile irons. (a, b) 60–40–18, 2.5 and 5 kW, respectively. (c, d) 80–55–06, 2.5 and 5 kW, respectively. (e, f) 100–70–03, 2.5 and 5 kW, respectively.

zone (F) and a hardened zone with a mixed martensite and ferrite structure (M + α).

The perlitic ductile iron (Fig. 10e, f), presents a martensitic hardened layer (M) and a molten zone (F). In this case we can obtain a surface hardened layer without melting.

The depth of the molten layer was similar in all three tested irons under the same operating conditions. The depths of the hardened zone were also similar in the ferritic–perlitic matrix ductile iron and in the perlitic iron using the same treatment.

In the three types of ductile iron, under conditions that lead to surface melting, superficial cracks appeared in the layer of white iron. The cracks were spaced regularly and ran across the tracks. The deeper the molten layer, the more abundant the cracks.

Fig. 11 shows a characteristic example of a series of cracks located on the zone treated with a 2.5 kW beam

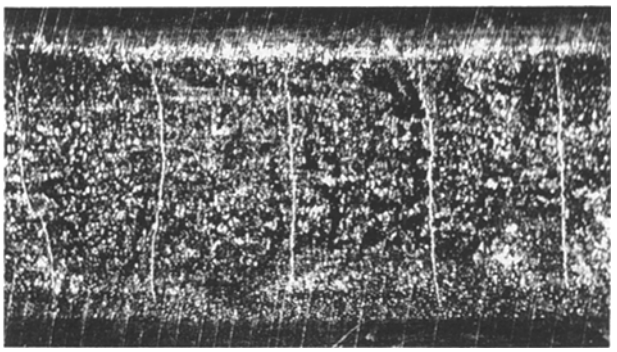

Figure 11 Transverse cracks on the solidified zone in the ferritic ductile iron. × 2.5

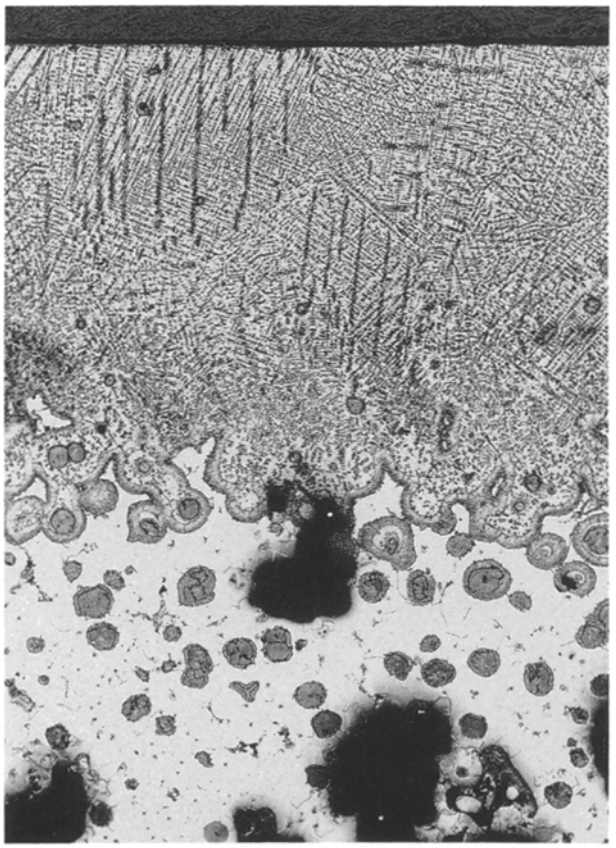

Figure 12 Porosity elimination by surface melting treatment. × 500

and 0.3 m min^{-1} scan rate. The molten layer has a depth of 0.43 mm.

In the absence of melting, the surface layer of the perlitic ductile iron transformed to martensite had no cracks, nor were there cracks in the martensitic portions obtained in the ferritic–perlitic matrix ductile iron.

The surface laser treatment also permitted superficial porosity to be eliminated. The micrograph in Fig. 12 illustrates the treatment of a ferritic ductile iron. There is accentuated porosity on the unmelted zone, while the porosity has disappeared completely near the surface.

4. Discussion

The laser surface treatment of ductile irons may be performed using superficial melting or martensitic hardening.

The surface melting treatment of the three test irons produced a layer of white iron with residues of graphite nodules which were partially dissolved. The degree of dissolution depended on melting time, temperature and nodule size.

The solidification structure depended on the operating conditions, and could be linked to the depth of the molten layer. In the molten layers with a depth of 0.2 mm or more, the degree of dissolution of the graphite nodules in the superficial zones was higher and the microstructure of the solidified material was eutectic. In the deeper zones, the graphite nodules only melted partially and the structure was hypoeutectic, the only one found in the molten layers with a depth of less than 0.2 mm.

The hardness of the white iron produced by laser treatment was above 1000 HV0.5 in all cases. The laser surface melting of the iron products permitted the porosity of the affected area to be eliminated. Cracks appeared, however, in the solidification process. To prevent this, it was necessary to preheat the iron at around 400 °C [11, 12].

The effect of martensitic hardening depends substantially on initial microstructure of the iron matrix. In the ferritic ductile iron, this martensitic treatment is not viable.

In the ferritic–perlitic matrix ductile iron, surface treatment without melting leads primarily to a transformation of the perlite into martensite. A small areola of martensite is formed around the graphite nodules, while most of the ferrite remains unaltered. Under these conditions, a continuous layer hardened to martensite cannot be obtained. In the tested perlitic iron, which had 15% ferrite around the graphite nodules, it was possible to obtain a continuous layer of martensite that kept the initial graphite nodules trapped. At an excessively high scan rate, a residue of ferrite could remain around the graphite nodules.

The laser hardening of ductile irons with perlitic and mixed perlitic–ferritic matrices produced a very hard martensite, around 860 HV0.5. No cracks appeared in the surface hardening of the perlitic ductile iron.

5. Conclusions

1. In the surface melt treatments of the ferritic, ferritic–perlitic and perlitic matrix irons, the layer of white iron obtained, composed of cementite, martensite and retained austenite, reached a similar depth when operating under the same conditions. The microstructure of the matrix thus had no significant effect on the melting process in the laser treatment. If the molten layer was deep ($\geqslant$ 0.2 mm), a eutectic type of solidification occurred, while lesser depths led to hypoeutectic solidification.

2. The white iron layer attained a hardness of more than 1000 HV0.5.

3. Melting permitted surface porosity to be eliminated. Transverse cracks appeared on the surface, spaced along the track, when the melting treatment was performed without preheating the samples.

4. Martensitic hardening was only partial in the ductile iron with a mixed ferritic–perlitic matrix. In the perlitic iron, surface hardening even permitted the ferritic fraction to be transformed to martensite.

5. The martensitic layers always had nodules of graphite that were practically undissolved. The hardness of the martensite derived from the perlite of the iron was around 860 HV0.5 in the zone affected by the treatment. These martensitic layers did not appear to have cracks.

Acknowledgement

This study was subsidized by the SEUI, CICYT Project PPA-86-0443-C02-02.

References

1. W. M. STEEN, ZHEN DA CHEN and D. R. F. WEST, in "Industrial Laser Annual Handbook" (Penn Well, Tulsa, OK, 1988) p. 80.
2. H. W. BERGMAN, *Surf. Eng.* **1** (1985) 137.
3. C. H. CHEN, C. P. LU and J. M. RIGSBEE, *Mater. Sci. Technol.* **4** (1988) 161.
4. A. GASSER, G. HERZIGER, E. W. KREUTZ and K. WISSENBARCH, in "Proceedings of LAMP' 87", Osaka, May, edited by Y. Arata (High Temperature Society of Japan, Osaka, Japan, 1987) p. 451.
5. B. L. MORDIKE, in "Advances in Surface Treatments", Vol. 5, edited by A. Niku-Lari (Pergamon Press, Oxford, 1987) p. 382.
6. K. MATHUR and P. A. MOLIAN, *J. Eng. Mater. Technol. Trans. ASME* **107** (1985) 200.
7. C. H. CHEN, C. P. LU and J. M. RIGSBEE, *Mater. Sci. Technol.* **4** (1988) 172.
8. P. W. LEECH, *Wear* **113** (1986) 233.
9. P. A. MOLIAN, *J. Eng. Mater. Technol. Trans. ASME* **109** (1987) 179.
10. J. RUIZ, B. J. FERNANDEZ and J. M. BELLO, in "Proceedings of the 2nd International Seminar on Surface Engineering with High Energy Beams", Science and Technology, Lisbon 1989, edited by CEMUL (Center of Mechanics and Materials of the Technical University of Lisbon, Lisbon, Portugal, 1989) p. 161.
11. G. RICCIARDI, F. PASQUINI and S. RUDILOSSO, in "Proceedings of the 1st Conference on Lasers in Manufacturing (LIM1)", Brighton, UK, November 1983, edited by M. Kimmit (IFS, Kempston, Bedford, UK, 1983) p. 87.
12. H. W. BERGMAN, in "Laser Surface Treatment of Metals", edited by C. W. Draper and P. Mazzoldi (Martinus Nijhoff, Dordrecht, Netherlands, 1986) p. 351.

Received 13 May 1993
and accepted 28 February 1994